

On Enhancing the Dissipative Behavior of Active Flux Advection Schemes

Christian Klingenberg^[0000-0003-2033-8204]

Simon Krotzsch^[0009-0003-1726-1610]

Philip Roe^[0000-0002-7596-2912]

In memory of Phil Roe

Abstract In this work, the traditional third-order Active Flux advection scheme is modified by reformulating the method and introducing additional parameters. The effect of these parameters is studied, leading to schemes with improved dissipative properties. These improvements are validated by numerical experiments.

Keywords Hyperbolic conservation laws · Active Flux · Semi-discrete method · Spectral error analysis

1 Introduction

Some 15 years ago Phil Roe introduced the Active Flux method [7], [8], [9], a numerical method for conservation laws, inspired by an idea of Bram van Leer [15]. It is a finite volume method. The degrees of freedom of the traditional third-order Active Flux version consist of cell averages and point values located at cell interfaces. These point values are evolved in time independently of the averages and are shared between two adjacent cells, resulting in a globally continuous reconstruction and hence a Riemann-solver-free method.

On April 26, 2026 Phil Roe passed away. Until the end of his life, he pursued the development of the Active Flux method with unwavering commitment. Examples of

Philip Roe

Christian Klingenberg
University of Würzburg, Institute of Mathematics, Emil-Fischer-Straße 40, Würzburg, 97074,
Germany, e-mail: christian.klingenberg@uni-wuerzburg.de

Simon Krotzsch
University of Würzburg, Institute of Mathematics, Emil-Fischer-Straße 40, Würzburg, 97074,
Germany, e-mail: simon.krotzsch@stud-mail.uni-wuerzburg.de

him pushing Active Flux forward are: in [11], the method was extended to advection–diffusion problems. An example of the connection to the superconvergence of DG methods was found in [12], and a practical comparison between the two approaches can be found in [13]. In [4] this comparison has now been expanded on. Furthermore, a high-order version was introduced in [14]. Phil Roe’s Active Flux work also inspired further contributions by other groups, some examples are [1], [5], [3], [2], [6].

The ICOSAHOM 2025 in Montréal was the last conference Phil Roe attended in person. In memory of Philip Roe, here we present one of his last ideas concerning the Active Flux method. First, the traditional third-order Active Flux method is reviewed and reformulated as an upwind method with correction terms depending on positive parameters. The dissipative and dispersive properties of this parameterized formulation are then analyzed, and parameter choices determined that yield methods with improved dissipative properties. Finally, numerical results are presented to further investigate the proposed methods and verify their enhanced properties.

2 The Active Flux method

We consider the third-order Active Flux method to solve the one-dimensional advection equation

$$\frac{\partial}{\partial t} q(t, x) + a \frac{\partial}{\partial x} q(t, x) = 0, \quad x \in \mathbb{R}, \quad t \in \mathbb{R}_+,$$

where $q : \mathbb{R}_+ \times \mathbb{R} \rightarrow \mathbb{R}$ and $a > 0$. Assume the computational domain is divided into grid cells $C_i = [x_{i-\frac{1}{2}}, x_{i+\frac{1}{2}}]$ of equal length $\Delta x > 0$. The midpoint of the cell C_i is denoted by x_i . The degrees of freedom of the traditional third-order Active Flux method are cell averages

$$Q_i(t) \approx \frac{1}{\Delta x} \int_{C_i} q(t, x) \, dx$$

and point values

$$q_{i+\frac{1}{2}}(t) \approx q(t, x_{i+\frac{1}{2}})$$

at the interfaces of the cells. Since point values are shared between adjacent cells, the degrees of freedom associated with the cell C_i are a point value and a cell average. If these values are given at some time $t^n = n\Delta t$ for all cells, the first step of the method is to fit a quadratic polynomial to the three degrees of freedom accessible per cell. An easy way to state this quadratic polynomial, which we call the reconstruction, is to consider a reference cell $[-\frac{\Delta x}{2}, \frac{\Delta x}{2}]$. The local reconstruction in cell C_i is defined as $q_{\text{recon},i} : [-\frac{\Delta x}{2}, \frac{\Delta x}{2}] \times [0, \infty) \rightarrow \mathbb{R}$,

$$q_{\text{recon},i}(t^n, \xi) = \frac{6Q_i(t^n) - q_{i+\frac{1}{2}}(t^n) - q_{i-\frac{1}{2}}(t^n)}{4} + \frac{q_{i+\frac{1}{2}}(t^n) - q_{i-\frac{1}{2}}(t^n)}{\Delta x} \xi + 3 \frac{q_{i-\frac{1}{2}}(t^n) + q_{i+\frac{1}{2}}(t^n) - 2Q_i(t^n)}{\Delta x^2} \xi^2,$$

where $\xi = x - x_i$ for $x \in C_i$. One can verify that this function interpolated the degrees of freedom, i.e.,

$$q_{\text{recon},i}\left(t^n, \pm \frac{\Delta x}{2}\right) = q_{i\pm\frac{1}{2}}(t^n), \quad \frac{1}{\Delta x} \int_{C_i} q_{\text{recon},i}^n(t^n, \xi) d\xi = Q_i(t^n).$$

From the integral of the conservation law, one can derive an update for the cell average:

$$Q_i(t^{n+1}) = Q_i(t^n) - \frac{a\Delta t}{\Delta x} \left(\bar{q}_{i+\frac{1}{2}}^{n+\frac{1}{2}} - \bar{q}_{i-\frac{1}{2}}^{n+\frac{1}{2}} \right),$$

where

$$\bar{q}_{i+\frac{1}{2}}^{n+\frac{1}{2}} = \frac{1}{\Delta t} \int_{t^n}^{t^{n+1}} q_{i+\frac{1}{2}}(t) dt \approx \frac{1}{\Delta t} \int_{t^n}^{t^{n+1}} q(t, x_{i+\frac{1}{2}}) dt.$$

To evaluate the integral, we use Simpson's rule:

$$\bar{q}_{i+\frac{1}{2}}^{n+\frac{1}{2}} = \frac{1}{6} \left(q_{i+\frac{1}{2}}(t^n) + 4q_{i+\frac{1}{2}}\left(t^n + \frac{1}{2}\Delta t\right) + q_{i+\frac{1}{2}}(t^n + \Delta t) \right).$$

The values $q_{i+\frac{1}{2}}(t^n + l\Delta t)$ for $l = \frac{1}{2}$ and $l = 1$ are obtained by solving the initial value problem at the locations of the point values, using the reconstruction as initial data. For the linear advection equation with $a > 0$, the solution is

$$q_{i+\frac{1}{2}}(t^n + l\Delta t) = q_{\text{recon},i}(t^n, \frac{\Delta x}{2} - al\Delta t),$$

under the assumption

$$\nu = \frac{a\Delta t}{\Delta x} \leq 1.$$

Note that since the update of the average is exact, this results in a third-order accurate method. For simplicity, define $Q_i^n = Q_i(t^n)$ and $q_{i\pm\frac{1}{2}}^n = q_{i\pm\frac{1}{2}}(t^n)$. The update formulas for the point values and the cell averages can be stated explicitly:

$$\begin{aligned} q_{i+\frac{1}{2}}^{n+1} &= (1-\nu)q_{i+\frac{1}{2}}^n + \nu q_{i-\frac{1}{2}}^n - 3\nu(1-\nu) \left((q_{i+\frac{1}{2}}^n - Q_i^n) - (Q_i^n - q_{i-\frac{1}{2}}^n) \right), \\ \bar{q}_{i+\frac{1}{2}}^{n+\frac{1}{2}} &= Q_i^n + (1-\nu) \left((1-\nu) (q_{i+\frac{1}{2}}^n - Q_i^n) + \nu (Q_i^n - q_{i-\frac{1}{2}}^n) \right), \\ Q_i^{n+1} &= Q_i^n - \nu \left(\bar{q}_{i+\frac{1}{2}}^{n+\frac{1}{2}} - \bar{q}_{i-\frac{1}{2}}^{n+\frac{1}{2}} \right). \end{aligned}$$

These explicit formulas can be interpreted as the first-order Upwind method applied separately to the cell average and the point values with additional correction terms. We can write these correction terms in a more general way by introducing parameters $R, S, T, U > 0$:

$$q_{i+\frac{1}{2}}^{n+1} = (1 - \nu)q_{i+\frac{1}{2}}^n + \nu q_{i-\frac{1}{2}}^n - \nu(1 - \nu)(R(q_{i+\frac{1}{2}}^n - Q_i^n) - S(Q_i^n - q_{i-\frac{1}{2}}^n)), \quad (1)$$

$$\bar{q}_{i+\frac{1}{2}}^{n+1} = Q_i^n + (1 - \nu)(T(q_{i+\frac{1}{2}}^n - Q_i^n) + U(Q_i^n - q_{i-\frac{1}{2}}^n)) \quad (2)$$

By choosing $R = S = 3$, $T = (1 - \nu)$ and $U = \nu$, one recovers the classical third-order scheme.

3 Spectral error analysis

The degrees of freedom of the method can be regarded as functions defined on a finite grid. Such functions can be decomposed into finite Fourier series in space at each time step t^n :

$$Q_i^n = \sum_{\theta} \hat{U}^n(\theta) e^{-\frac{1}{2}I\theta} e^{I(i+\frac{1}{2})\theta}$$

and

$$q_{i+\frac{1}{2}}^n = \sum_{\theta} \hat{q}^n(\theta) e^{I(i+\frac{1}{2})\theta},$$

where I is the imaginary unit and $\theta = k\Delta x$ the phase angle with wavenumber k . For convenience, we define a new amplitude for the cell averages, $\hat{Q}^n(\theta) = \hat{U}^n(\theta) e^{-\frac{1}{2}I\theta}$. Assume that the average and point values are given by a single harmonic, i.e.,

$$Q_i^n = \hat{Q}^n(\theta) e^{I(i+\frac{1}{2})\theta}.$$

The exact time evolution of the point values and cell averages is given by

$$q(t^{n+1}, x_{i+\frac{1}{2}}) = q(t^n, x_{i+\frac{1}{2}}) e^{-I\theta\nu},$$

$$\frac{1}{\Delta x} \int_{C_i} q(t^{n+1}, x) dx = \frac{1}{\Delta x} \int_{C_i} q(t^n, x) dx e^{-I\theta\nu}$$

Evolving the degrees of freedom in time with the parameterized version of the Active Flux scheme yields

$$\hat{q}^{n+1} = (1 - \nu)\hat{q}^n + \nu\hat{q}^n e^{-I\theta} - \nu(1 - \nu) \left(R(\hat{q}^n - \hat{Q}^n) - S(\hat{Q}^n - \hat{q}^n e^{-I\theta}) \right)$$

and

$$\begin{aligned}\hat{Q}^{n+1} &= \hat{Q}^n e^{-\frac{1}{2}I\theta} - \nu \left(\hat{Q}^n + (1-\nu) \left(T(\hat{q}^n - \hat{Q}^n) + U(\hat{Q}^n - \hat{q}^n e^{-I\theta}) \right) \right. \\ &\quad \left. - \hat{Q}^n e^{-I\theta} + (1-\nu) \left(\left(T(\hat{q}^n - \hat{Q}^n) + U(\hat{Q}^n - \hat{q}^n e^{-I\theta}) \right) e^{-I\theta} \right) \right).\end{aligned}$$

For simplicity, we omit the dependence on θ . The amplification matrix $A \in \mathbb{C}^{2 \times 2}$ of this scheme, i.e., the matrix that satisfies

$$\begin{pmatrix} \hat{Q}^{n+1} \\ \hat{q}^{n+1} \end{pmatrix} = A \begin{pmatrix} \hat{Q}^n \\ \hat{q}^n \end{pmatrix},$$

is

$$A = \begin{pmatrix} 1 - \nu(1 + (1-\nu)(U-T))(1 - e^{-I\theta}) & \nu(1-\nu)(Ue^{-I\theta} - T)(1 - e^{-I\theta}) \\ \nu(1-\nu)(R+S) & (1-\nu)(1-\nu R) + \nu(1 - (1-\nu)S)e^{-I\theta} \end{pmatrix}.$$

Mathematica [16] allows us to compute the eigenvalues of A as power series in θ . The first two terms in the expansion of the first eigenvalue, which we will also call the principal eigenvalue, are 1 and $-I\nu\theta$, while higher order terms in θ depend on the positive parameters R , S , T , and U . In contrast, all terms of the second (spurious) eigenvalue depend on these parameters. The principal eigenvalue describes the behavior of low frequencies and the spurious eigenvalue governs the behavior of high frequencies. The exact eigenvalue is

$$\lambda_{\text{exact}} = e^{-I\nu\theta} = \sum_{j=0}^{\infty} \frac{(-I\nu\theta)^j}{j!}.$$

Hence, the first two terms of the principal eigenvalue match the terms of the exact eigenvalue. We can determine the parameters R , S , T , U such that the principal eigenvalue is exact up to the highest possible order of θ . This can be done by employing Mathematica [16]. The resulting conditions on the parameters to obtain a principal eigenvalue which is second-order correct are:

$$U = \frac{R - 2ST + S}{2R}, \quad (3)$$

or

$$R = 0 \quad \text{and} \quad T = \frac{1}{2}. \quad (4)$$

To obtain a third-order correct eigenvalue, the parameters must satisfy

$$T = -\frac{1}{3}(\nu + 1)R + \frac{R^2}{R+S} + \frac{1}{2} \quad \text{and} \quad U = \frac{1}{6} \left(2S \left(\nu - \frac{3R}{R+S} + 1 \right) + 3 \right). \quad (5)$$

If conditions (5) are satisfied, the difference between the exact and principal eigenvalue is

$$\lambda_1 - \lambda_{\text{exact}} = \frac{1}{72}(\nu - 1)\nu \left((\nu - 2)(\nu + 1) + \frac{18}{R + S} \right) \theta^4 + O(\theta^5).$$

If $R = S = 3$, conditions (5) reduce to $T = 1 - \nu$ and $U = \nu$, which are the parameters corresponding to the traditional Active Flux method. The conditions for a fourth-order correct eigenvalue are

$$\begin{aligned} S &= \frac{18}{-\nu^2 + \nu + 2} - R, \\ T &= \frac{1}{18}(9 - (\nu + 1)R((\nu - 2)R + 6)), \\ U &= \frac{1}{18} \left(-((\nu - 2)(\nu + 1)R^2) - 6(\nu + 4)R + \frac{9(\nu - 14)}{\nu - 2} \right). \end{aligned} \quad (6)$$

The error of the principal eigenvalue is in this case

$$\lambda_1 - \lambda_{\text{exact}} = \frac{1}{540}i\nu \left(2\nu^4 - 5\nu^3 + 5\nu - 2 \right) \theta^5 + O(\theta^6).$$

This error does not depend on any of the parameters and hence it is not possible to obtain a fifth-order correct eigenvalue with the right parameter choice. Nevertheless, if $\nu = 0$, $\nu = 1$ or $\nu = \frac{1}{2}$, the fifth-order error term vanishes. For $\nu = 0$ and $\nu = 1$, this is the expected behavior, since the method is exact for these values of ν , independently of the chosen parameter. If $\nu = \frac{1}{2}$, conditions (6) simplify to

$$S = 8 - R, \quad T = \frac{1}{8}(R - 2)^2, \quad U = \frac{1}{8}(R - 6)^2. \quad (7)$$

It is a simple matter of calculation to show that for a scheme with parameters that satisfy (7) and $\nu = \frac{1}{2}$,

$$q_{i+\frac{1}{2}}^{n+2} = q_{i-\frac{1}{2}}^n \quad \text{and} \quad Q_i^{n+2} = Q_{i-1}^n.$$

Therefore, conditions (6) yield a scheme that is exact for $\nu = \frac{1}{2}$. Alternatively, imposing conditions (5) with $S = 8 - R$ also leads to a scheme that is exact for $\nu = \frac{1}{2}$, since these conditions reduce to conditions (7). The principal eigenvalue of these schemes matches the exact eigenvalue,

$$\lambda_1 = e^{-I\frac{\theta}{2}}, \quad (8)$$

and the spurious eigenvalue is

$$\lambda_2 = -e^{-I\frac{\theta}{2}}.$$

That these schemes are exact for $\nu = \frac{1}{2}$ is not an arbitrary result, but a consequence of the amplification matrix. The elements of the amplification matrix consist of terms

$$ce^{-nI\theta}$$

with $n \in \mathbb{N}_0$ and $c \in \mathbb{R}$. If the amplification matrix is in \mathbb{R} (in this case we also call it the amplification factor), for example, for a finite volume method, then the eigenvalue of A , which is in this case just A , can only be of the form $e^{-nI\theta}$ multiplied by some real factor. Hence, an eigenvalue like (8) is not possible. If $A \in \mathbb{R}^{2 \times 2}$, then the eigenvalues are the zeros of the characteristic polynomial, which is, in this case, a quadratic polynomial. Therefore, square root terms can appear in the eigenvalues, and these root terms are the reason why eigenvalues consisting of terms $e^{-\frac{n}{2}I\theta}$ multiplied by some real factor can appear. With this argument, we expect that it is possible to modify higher order schemes to obtain methods that are exact for different values of ν .

Next, we analyze the dissipation and dispersion behavior of the schemes for certain parameter choices. Given the amplification matrix, we can define the dispersion and dissipation error in the spirit of [10]. The dissipation error (or relative amplitude) \mathcal{E}_1 is defined as

$$\mathcal{E}_1(\nu, \theta) = \left(\frac{|\lambda_1(\nu, \theta)|}{|\lambda_{\text{exact}}(\nu, \theta)|}, \frac{|\lambda_2(\nu, \theta)|}{|\lambda_{\text{exact}}(\nu, \theta)|} \right)^T,$$

and the dispersion error (or relative wave speed) \mathcal{E}_2 is defined as

$$\mathcal{E}_2(\nu, \theta) = \left(\frac{\phi_1(\nu, \theta)}{\phi_{\text{exact}}(\nu, \theta)}, \frac{\phi_2(\nu, \theta)}{\phi_{\text{exact}}(\nu, \theta)} \right)^T,$$

where $\phi_j(\nu, \theta)$ is the phase of the eigenvalue $\lambda_j(\nu, \theta)$ with $j = 1, 2$ and $\phi_{\text{exact}}(\nu, \theta)$ is the phase of $\lambda_{\text{exact}}(\nu, \theta)$. We will focus our analysis on the schemes that have an at least third-order accurate principal eigenvalue, starting with schemes that have a fourth-order correct eigenvalue. Imposing conditions (6) results in eigenvalues

$$\lambda_{1,2} = \frac{2(2\nu - 1)\nu e^{-I\theta}}{\nu + 1} - 4\nu - \frac{6}{\nu - 2} - 2 \pm \frac{3(\nu - 1)\nu e^{-2I\theta}}{(\nu - 2)(\nu + 1)} \sqrt{e^{3I\theta} (3I(2\nu - 1) \sin(\theta) + (1 - 2\nu)^2 \cos(\theta) - 4(\nu - 2)(\nu + 1))}.$$

The dissipation and dispersion errors are always the same, no matter the choice of R . A useful way to determine R seems to make the expressions for the other parameters as simple as possible. The choice

$$R = \frac{6}{2 - \nu}$$

accomplishes this, yielding

$$S = \frac{6}{1 + \nu}, \quad \text{and} \quad T = U = \frac{1}{2}.$$

Imposing conditions (5), yields the eigenvalues

$$\begin{aligned} \lambda_{1,2} = & 1 + \frac{1}{6}\nu \left(\nu^2(R+S) - e^{-I\theta}((\nu-2)(\nu-1)(R+S) - 6) - (R+S) - 6 \right. \\ & \pm \frac{1}{R+S} \left((\nu-1)e^{-2I\theta} \left(e^{3I\theta}(R+S)^3(3I(2\nu-1)(R+S)\sin(\theta) \right. \right. \\ & \left. \left. + \cos(\theta)((2(\nu-1)\nu+5)(R+S) - 36) - 2(\nu-2)(\nu+1)(R+S) + 36 \right)^{\frac{1}{2}} \right) \left. \right). \end{aligned}$$

Both eigenvalues depend only on $(R+S)$. We set $R=S$ and consider the resulting schemes as a class depending on a single parameter R . We refer to the scheme with a fourth-order accurate eigenvalue as Scheme 4 and to the class of schemes with third-order accurate eigenvalues as Scheme 3.

The dissipation error of Scheme 4 and Scheme 3 with $R=2$, $R=3$ (traditional Active Flux) and $R=4$ with respect to θ , can be seen in Figure 1 for different values of ν . In Figure 2, one can see the dispersion error of the principal eigenvalue with respect to θ . A method with a perfect dissipative and dispersive behavior would have a dissipation and dispersion error of 1. Scheme 4 and Scheme 3 with $R=4$ have improved dissipative behavior compared to the traditional third-order scheme. This advantage appears to come with a cost, since these schemes are more dispersive than the classical version of the Active Flux scheme. Scheme 3 with $R=2$ is more dissipative than the traditional Active Flux method. The relative wave speed for the difference values of ν is in some sense the opposite to the one of the traditional method. For example, for $\nu=0.1$ the dispersion error of the traditional method is larger than one, and for Scheme 3 with $R=2$ it is smaller than one, provided $|\theta|$ is sufficiently large.

The parameter R in Scheme 3 allows us to adjust the dissipative/dispersive behavior of the method in some sense. Starting with $R=3$ and increasing R gives us a method that has an improved dissipative behavior compared to the classical Active Flux method and decreasing R leaves us with a method that has an inferior dissipative behavior.

4 Numerical results

For the numerical test, we choose $a=1$ and consider $[-5,5]$ as the computational domain, divided into 100 cells. We impose periodic boundary conditions. As a first numerical experiment, we consider a high-frequency sine wave as initial data and compute the numerical solution with Scheme 4 and Scheme 3 with $R=2, 3$, and 4 at $T=1000$. The numerical solution compared to the exact solution at this time is depicted in Figure 3. The Amplitude of the waves of the numerical solutions computed with Scheme 3 with $R=2$ and $R=3$ is (almost) zero, while Scheme 3 ($R=4$) retains approximately 75 percent and Scheme 4 almost 100 percent of the original amplitude. Figure 4 shows the numerical results for a square wave. Unfortunately, oscillations appear near the discontinuities for the methods with improved dissipative behavior and, as a consequence, worsened dispersive behavior. Scheme 3 with $R=2$ and $R=3$ experiences a small overshoot, but is overall able to deal better with the discontinuities.

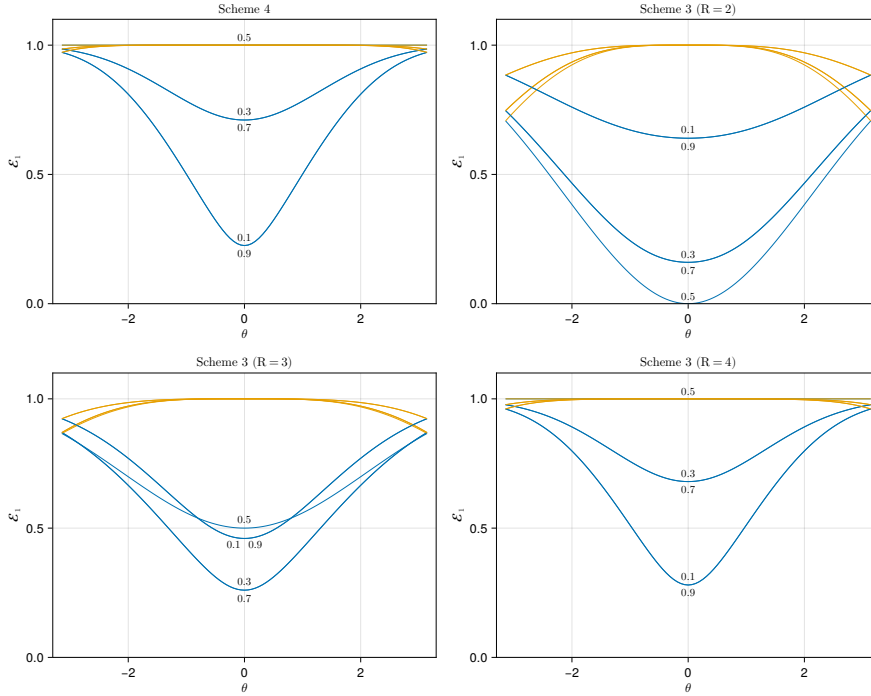


Fig. 1 The dissipation error \mathcal{E}_1 with respect to θ for different values of ν . The orange curves represent the error corresponding to the principal eigenvalue.

The same results are visible in Figure 5, where the initial data consists of three different shapes.

Experimentally, values of $R \in [3, 4]$ can be determined for which the oscillations remain acceptable. For example, in Figure 6 one can see the results for $R = 3.75$ at $T = 10$ and $T = 100$. There are some overshoots, but no oscillations. Furthermore, the sharp spike is better resolved compared to the classical Active Flux method (Figure 5). As theoretically expected, Scheme 4 and Scheme 3 with $R = 4$ are exact for $\nu = 0.5$ (see Figure 7).

5 Conclusion and outlook

In this work, we presented a reformulation of the traditional third-order Active Flux method as an upwind scheme with parameter-dependent correction terms. This formulation enables the selection of parameters, leading to a scheme with significantly improved dissipative behavior (Scheme 4), as well as a class of schemes depending on a single parameter that allows control over the dissipative behavior (Scheme 3). These results were verified by numerical experiments.

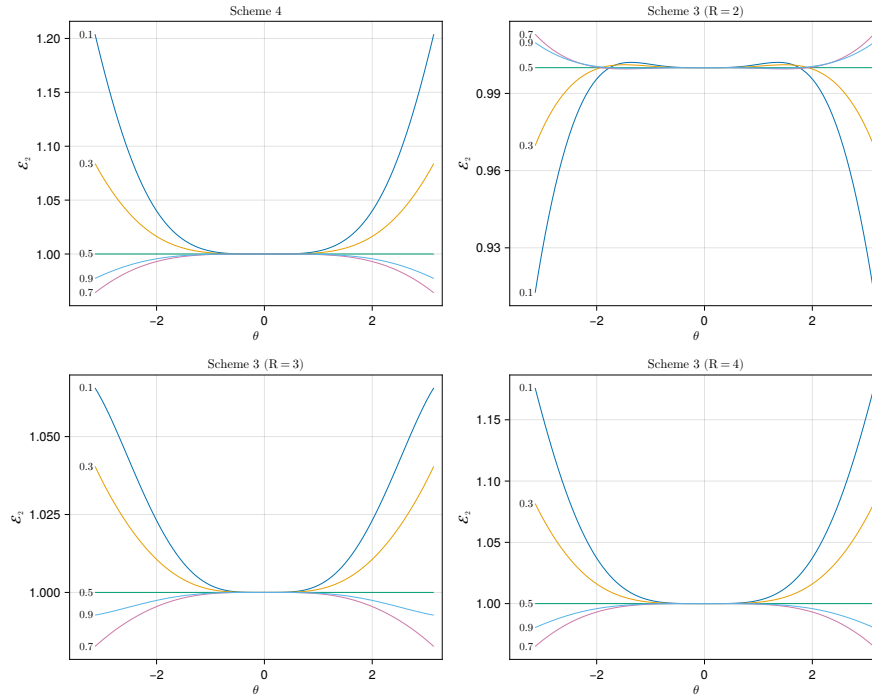


Fig. 2 The first component of the dispersion error \mathcal{E}_2 corresponding to the principal eigenvalue with respect to θ for different values of ν .

A topic of future work is to extend this idea to linear systems in one and two spatial dimensions, possibly to non-linear conservation law as well as to higher order Active Flux methods.

Acknowledgement

We acknowledge Lisa Lechner and Wasilij Barsukow for inspiring and productive discussions.

Competing Interests

The authors have no conflicts of interest to declare that are relevant to the content of this chapter.

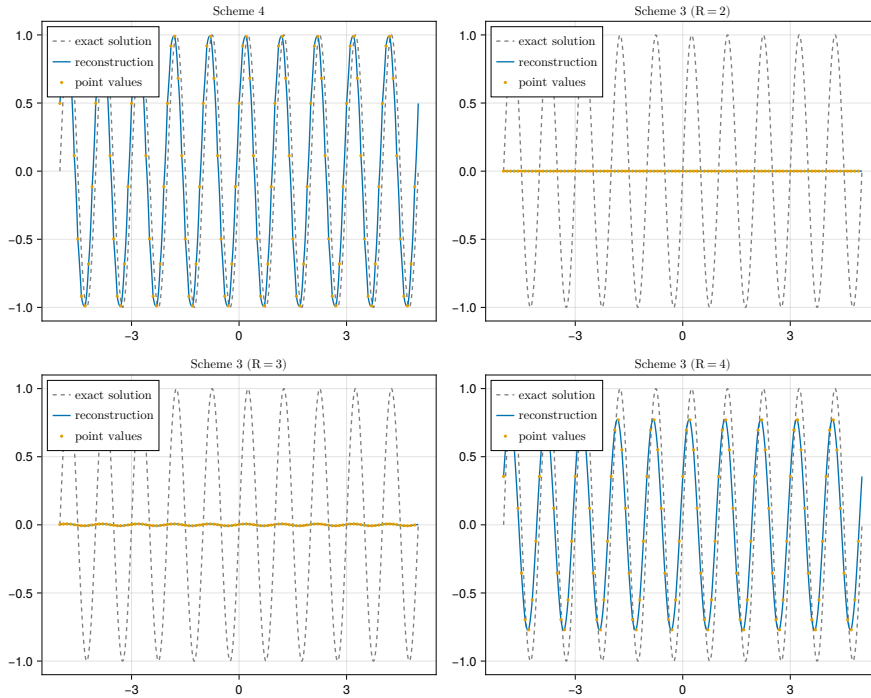


Fig. 3 The numerical solution computed with the different methods with $\nu = 0.7$ at $T = 1000$ in comparison to the analytical solution.

References

1. Abgrall, R., Boscheri, W., Liu, Y.: Virtual finite element and hyperbolic problems: The PAMPA algorithm. *J. Comput. Phys.* (2026) doi: 10.1016/j.jcp.2025.114521
2. Barsukow, W.: An active flux method for the Euler equations based on the exact acoustic evolution operator. *arXiv preprint* (2025) doi: 10.48550/arXiv.2506.03291
3. Barsukow, W., Hohm, J., Klingenberg C., Roe, P.: The Active Flux Scheme on Cartesian Grids and Its Low Mach Number Limit. *J. Sci. Comput.* (2019) doi: 10.1007/s10915-019-01031-z
4. Barsukow, W., Klingenberg C., Krotzsch, S.: On the equivalence of semi-discrete Active Flux and Discontinuous Galerkin methods and a comparison of their performance. *arXiv preprint* (2026) doi: 10.48550/arXiv.2603.18160
5. Chudzik, E., Helzel, C. (2023). A Review of Cartesian Grid Active Flux Methods for Hyperbolic Conservation Laws. In: Franck, E., Fuhrmann, J., Michel-Dansac, V., Navoret, L. (eds) *Finite Volumes for Complex Applications X—Volume 1, Elliptic and Parabolic Problems*, pp. 93–109, Springer, Cham (2023)
6. Duan, J., Chandrashekar, P., Klingenberg, C.: Active flux for ideal magnetohydrodynamics: A positivity-preserving scheme with the Godunov-Powell source term. *arXiv preprint* (2025) doi: 10.48550/arXiv.2506.04857
7. Eymann, T., and Roe, P.: Active Flux Schemes. In: 49th AIAA Aerospace Science meeting (2011) doi: 10.2514/6.2011-382
8. Eymann, T., Roe, P.: Active Flux Schemes for Systems. In: 20th AIAA Computational Fluid Dynamics Conference (2011) doi: 10.2514/6.2011-3840

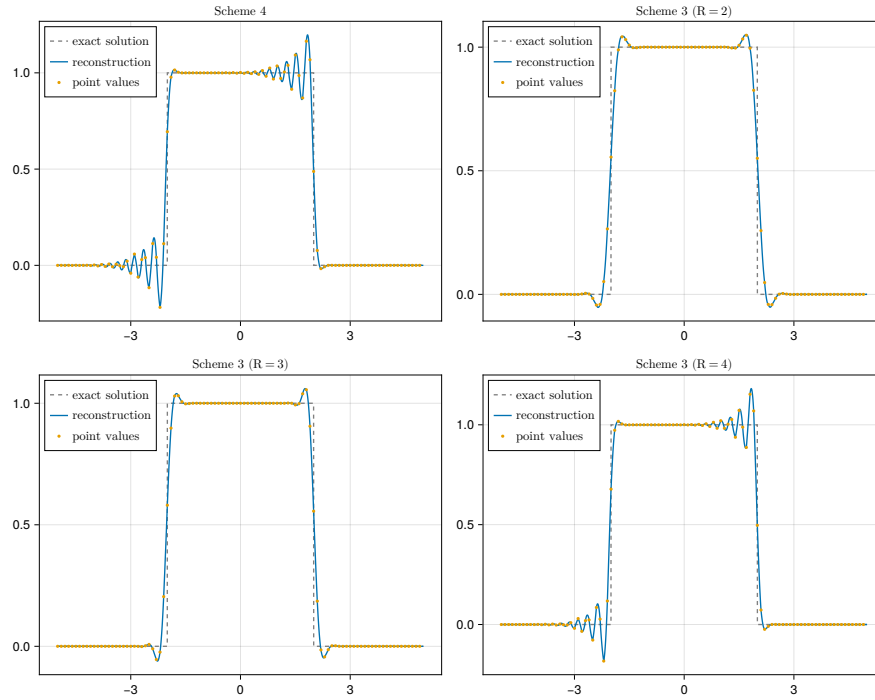


Fig. 4 The numerical solution computed with the different methods with $\nu = 0.7$ at $T = 10$ in comparison to the analytical solution.

9. Eymann, T., Roe, P.: Multidimensional Active Flux Schemes. In: 21st AIAA Computational Fluid Dynamics Conference (2013) doi: 10.2514/6.2011-382
10. Hirsch, C.: Numerical Computation of Internal and External Flows, 2nd ed. Butterworth-Heinemann, Oxford (2007)
11. Nishikawa, H., Roe, P.: Third-order active-flux scheme for advection diffusion: Hyperbolic diffusion, boundary condition, and Newton solver. *Comput. & Fluids* (2016) doi:10.1016/j.compfluid.2015.10.020
12. Roe, P.: A simple explanation of superconvergence for discontinuous Galerkin solutions to $u_t + u_x = 0$. *Commun. Comput. Phys.* (2017) doi: 10.4208/cicp.OA-2016-0052
13. Roe, P., Maeng, J., Fan, D.: Comparing active flux and discontinuous Galerkin methods for compressible flow. In: 2018 AIAA Aerospace Sciences Meeting (2018) doi:10.2514/6.2018-0836
14. Samani, I., Roe, P.: Acoustics on a Coarse Grid. In: AIAA SCITECH 2023 Forum (2023) doi:10.2514/6.2023-1156
15. Van Leer, B.: Towards the ultimate conservative difference scheme IV: A new approach to numerical convection," *J. Comput. Phys.* (1977) doi: 10.1016/0021-9991(77)90095-X
16. Wolfram Research, Inc., Mathematica, Version 14.3, Champaign, IL, 2025

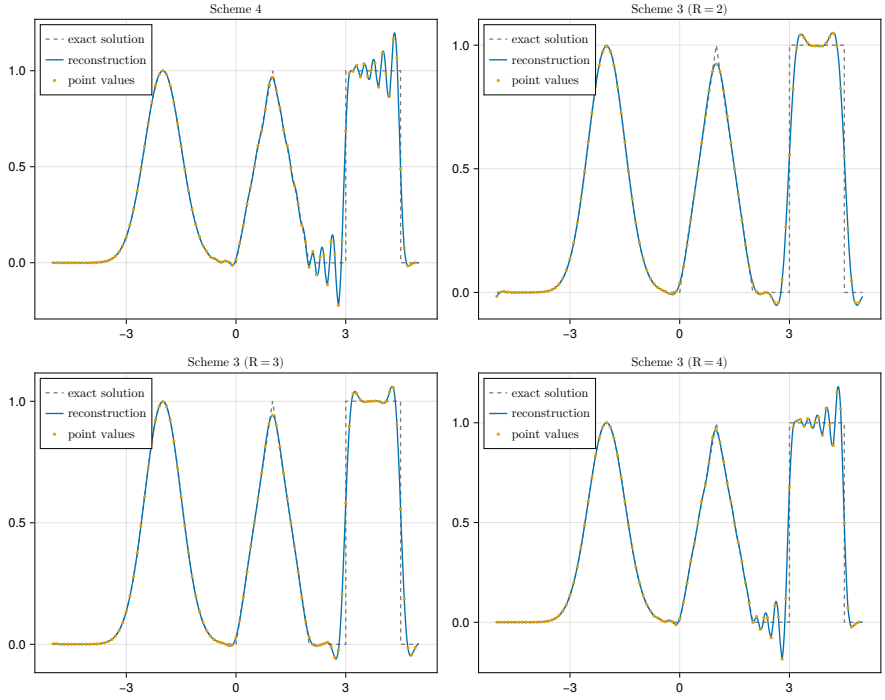


Fig. 5 The numerical solution computed with the different methods with $\nu = 0.7$ at $T = 10$ in comparison to the analytical solution.

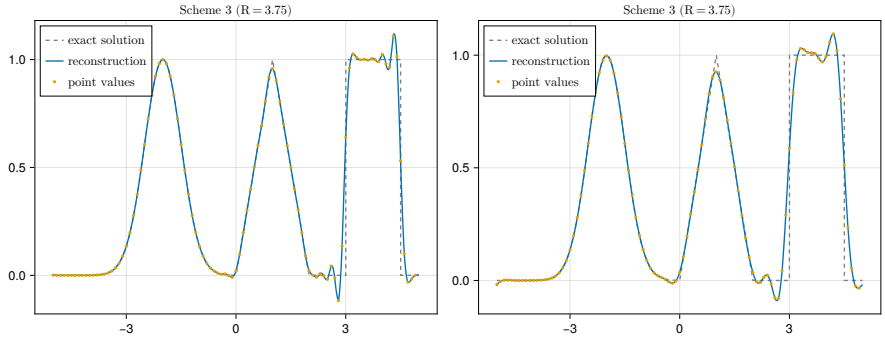


Fig. 6 The numerical solution computed with Scheme 3 ($R = 3.75$) with $\nu = 0.7$ at $T = 10$ (left) and $T = 100$ (right) in comparison to the analytical solution.

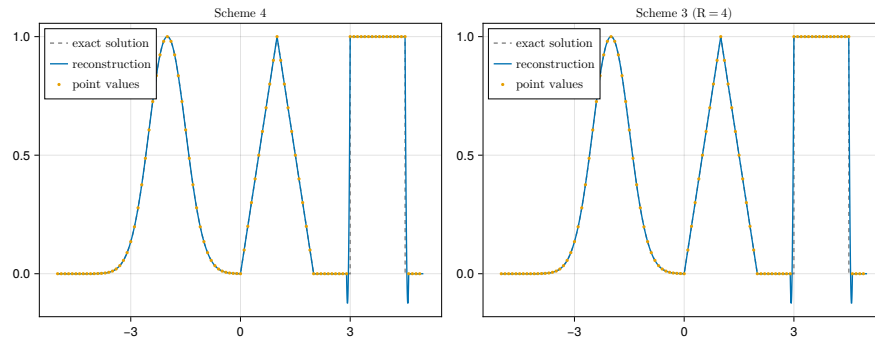


Fig. 7 The numerical solution computed with the different methods with $\nu = 0.5$ at $T = 10$ in comparison to the analytical solution.